Available online at www.sciencedirect.com
ScienceDirect
Superlattices and Microstructures 41 (2007) 7–16
Superlattices and Microstructures
www.elsevier.com/locate/superlattices

Dynamical behavior and cut-off frequency of Si/SiGe microcoolers

Y. Ezzahri[a,b,*], S. Dilhaire[a], L.D. Patiño-Lopez[a], S. Grauby[a], W. Claeys[a], Z. Bian[b], Y. Zhang[b], A. Shakouri[b]

[a] *Centre de Physique Moléculaire optique et Hertzienne (CPMOH), Université Bordeaux 1, 351, cours de la libération, 33405 Talence cedex, France*

[b] *Jack Baskin School of Engineering, University of California at Santa Cruz, Santa Cruz, CA 95064-1077, USA*

Received 22 February 2006; received in revised form 4 July 2006; accepted 22 August 2006
Available online 2 October 2006

Abstract

Solid-state microcoolers offer an attractive way to solve some of the problems related to temperature stabilisation and control, not only in optoelectronic and microelectronic applications, but also in biological applications where specimens require cooling. One of the important parameters of these coolers is their transient response or their cut-off frequency. We studied how this parameter is influenced by material properties (e.g., substrate and superlattice layer thermal diffusivities), and by geometrical factors (e.g., microcooler cross sectional area or thickness). Our models are based on a modified Thermal Quadrupole Method, which only takes the Peltier effect into account; the reason behind the modification is that the Peltier and Joule effects are uncorrelated in the frequency domain, so their contributions can be studied separately. The thermophysical properties of the microcooler are assumed to be temperature independent. The effect of the top side heat leakage on the performance of the microcooler is also presented.

Keywords: Superlattice; Microcooler; Thermoelectric; Thermionic; Cut-off frequency; Thermal quadrupole method

1. Introduction

Excess heat generation and thermal management problems have grown with the rapid development of VLSI technology, creating barriers to increasing clock speeds and decreasing feature sizes in optoelectronic and microelectronic applications. Because of their bulk manufacturing process, their small cooling power density and their slow transient response, on

* Corresponding author at: Jack Baskin School of Engineering, University of California at Santa Cruz, Santa Cruz, CA 95064-1077, USA. Tel.: +1 831 459 1292; fax: +1 831 459 4829.
E-mail address: younes@soe.ucsc.edu (Y. Ezzahri).

0749-6036/$ - see front matter
doi:10.1016/j.spmi.2006.08.006

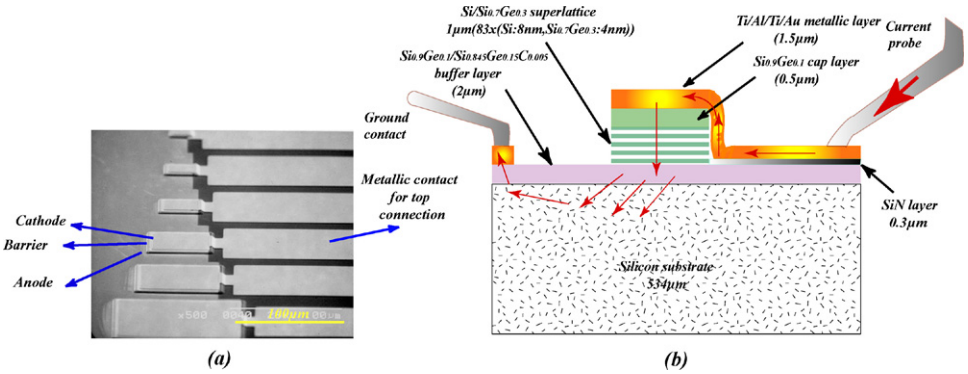

Fig. 1. (a) SEM picture of microcoolers, and (b) schematic diagram of the microcooler cross section. Arrows indicate the electrical current conventional direction.

the order of a few seconds, on-chip cooling and hot spot removal are beyond the capability of the conventional Bi_2Te_3 thermoelectric coolers. Due to an increasing demand for localized cooling and temperature stabilization in microelectronic and optoelectronic devices in the last ten years, microrefrigerator devices have attracted a lot of attention; moreover, the possibility of using integrated thermoelectric refrigeration to cool down biological specimens in vitro has increased demand. Superlattices and low dimensional materials have manifested very interesting thermoelectric properties, enabling them to have a figure of merit ZT exceeding 1 at room temperature. SiGe is a good thermoelectric material at high temperatures and SiGe/Si superlattices have been used to enhance cooling performance at room temperatures [1]. Si-based microcoolers are attractive for their potential monolithic integration with Si microelectronics. Recently some models have been reported to simulate the performance of these microcoolers in both the DC and AC regimes [2–4]. In this paper, the Thermal Quadrupole Method (TQM) [5] is used to simulate the dynamical behavior and cut-off frequency of Si/SiGe microcooler devices, and to study how the latter parameter is influenced by material properties (e.g., substrate and Si/SiGe superlattice thermal diffusivities), and by geometrical factors (e.g., microcooler cross sectional area or thickness). The effect of the top side heat leakage is also studied. The thermophysical properties of the microcooler are assumed to be temperature independent. This method has been used with great success to model the behavior of a conventional thermoelectric couple (Bi_2Te_3) [6], and more recently Si/SiGe microcoolers [4]. It consists of an analytical model which predicts electric and thermal responses at the first and second harmonic, thus making it possible to distinguish, in the case of a pure sine wave electrical excitation, the Peltier effect from the Joule effect. The first appears at the same frequency as the operating current, whereas the second appears at double this frequency. Since the frequency-dependent measurements are quite precise, they could be applied in the characterization of thermoelectric material properties.

2. Sample description

Fig. 1(a) shows a Scanning Electron Microscope picture of a set of Si/SiGe microcoolers with five different sizes. Fig. 1(b) illustrates a schematic cross sectional view of a real Si/SiGe superlattice microcooler we have considered in our simulation. It is constituted of a 1 μm thick superlattice layer with a structure of 83 × (8 nm Si/4 nm $Si_{0.7}Ge_{0.3}$) and doping concentration of 5×10^{19} cm^{-3}. The buffer layer is a 1 μm thick $Si_{0.9}Ge_{0.1}$ film followed by a 1 μm

thick $Si_{0.9}Ge_{0.1}/Si_{0.845}Ge_{0.15}C_{0.005}$ superlattice with the same doping concentration as the superlattice. The cap layer is 0.5 μm in total, consisting of a 0.25 μm $Si_{0.9}Ge_{0.1}$ film with a doping concentration of 5×10^{19} cm^{-3} followed by another 0.25 μm film with a higher doping concentration of 2×10^{20} cm^{-3} [7]. The most important part of the device is the superlattice layer. In addition to thermionic emission, it can also reduce the thermal conductivity which helps to prevent the heat to flow back to the cold junction from the substrate. The buffer layer on top of the Si substrate was included in order to reduce the lattice mismatch strain between the substrate and the superlattice [8]. The cap layer with the higher doping concentration of 2×10^{20} cm^{-3} was included in order to improve the ohmic contact between the metal and the semiconductor. The SiN insulating layer is added to prevent any current leaking from the probe into the substrate, thus the current path is confined from the probe to the top of the superlattice before being distributed into the substrate. The superlattice was grown in a molecular beam epitaxy (MBE) machine on a five inch diameter (001)-oriented Si substrate, and p-type doped to 0.003–0.007 Ω cm with boron. A 1.5 μm Ti/Al/Ti/Au layer was evaporated on top of the sample for electrical contact.

3. Thermoelectric and thermionic cooling

In a Si/SiGe microcooler, Peltier cooling occurs at the metal layer/cap layer junction and buffer layer/substrate junction when the device is fed by a current. The density of heat that can be exchanged with the surrounding medium is characterized by the effective Seebeck coefficient at these junctions, and it is proportional to both current intensity and junction temperature.

Assuming small current densities, we can define an effective Seebeck coefficient for thermionic cooling (similar to conventional thermoelectric cooling). The density of heat can be considered as linearly dependent on the current [9,10]. In our model, we assume that the Seebeck coefficient value takes into account both thermoelectric and thermionic phenomena.

4. Theoretical model and simulation

Our theoretical model is based on the TQM. The thicknesses of the different layers, including the superlattice layer, are several orders of magnitude larger than the mean free path of both electrons and phonons. Hence, we can assume a diffusive regime, and the Fourier Diffusive Classical Heat Equation (FDCHE) can be applied to describe heat transport inside the sample. The thickness of the whole structure is very small compared to that of the substrate; moreover, all Peltier sources are uniform on all junction plans, the heat transfer across the sample can be considered one-dimensional in the cross-plan direction of the device. We will assume the conditions are adiabatic and neglect both the side and surface losses caused by convection–radiation. This can be justified due to the small dimensions of the microcooler and marginal cooling temperature reduction. Our structure is formed of four essential layers.

In adiabatic conditions, the resolution of the FDCHE in a passive, linear, isotropic, and homogeneous medium for a one-dimensional heat transfer with the Laplace transform gives a linear relation between temperature-flux vectors at both ends. The transfer matrix of each layer can be put in the form:

$$\begin{pmatrix} \theta_{\text{in}} \\ \phi_{\text{in}} \end{pmatrix} = \begin{pmatrix} A & B \\ C & D \end{pmatrix} \begin{pmatrix} \theta_{\text{out}} \\ \phi_{\text{out}} \end{pmatrix} = \begin{pmatrix} ch(qe) & \frac{1}{K} sh(qe) \\ K sh(qe) & ch(qe) \end{pmatrix} \begin{pmatrix} \theta_{\text{out}} \\ \phi_{\text{out}} \end{pmatrix} = M \begin{pmatrix} \theta_{\text{out}} \\ \phi_{\text{out}} \end{pmatrix} \tag{1}$$

where $q = \sqrt{\frac{p}{\alpha}}$, p is Laplace parameter, $K = \beta \Sigma q$, and $\alpha = \frac{\beta}{\rho C}$ is the thermal diffusivity of the medium, β, ρC, e and Σ are respectively thermal conductivity, specific heat per unit volume, thickness, and area of the plan isothermal surface of the medium.

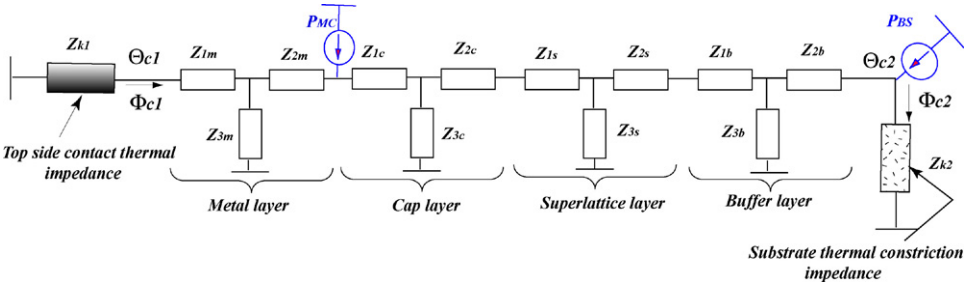

Fig. 2. Thermal quadrupole system of the Si/SiGe microcooler when only Peltier sources are considered.

The characteristics of this matrix, namely $A = D$, and $\mathrm{Det}(M) = 1$, are typical for a transfer matrix of a symmetrical system. Such a system remains unchanged if one reverses the axis of propagation, and can be related to the properties of a passive four-terminal network, which can be represented by three impedances connected in the "T" circuit, as shown in Fig. 2, which represents the quadrupole system of all microcoolers. We must note here that the ground level corresponds to room temperature, the impedances are thermal, and they are a function of the transfer matrix coefficients:

$$Z_1 = Z_2 = \frac{A-1}{C}, \qquad Z_3 = \frac{1}{C}. \tag{2}$$

This representation by impedances corresponds to the relation between boundary conditions. We suppose that the sample is excited with a pure sine wave current of frequency f:

$$I(t) = I_e \cos(2\pi f t). \tag{3}$$

The flow of current gives rise to two effects: the Peltier effect which appears at the same frequency of excitation f, and the Joule effect which appears at double this frequency $2f$. The two effects are uncorrelated in Fourier space. We can thus use the principle of superposition, and analyze electrical and thermal responses produced at each frequency separately. We first focus only on the Peltier effect and consider the response at the first harmonic. The application of Kirchhoff laws to the quadrupole system of Fig. 2 allows us to get a matrix relation, which represents the heat transfer for the whole structure in Laplace space, between $\binom{\theta_{C1}}{\phi_{C1}}$ and $\binom{\theta_{C2}}{\phi_{C2}}$, the temperature-flux vectors at the top metal layer, and the interface buffer-layer/substrate respectively, when only Peltier sources are considered:

$$\begin{pmatrix}\theta_{C1}\\ \phi_{C1}\end{pmatrix} = M_M M_C M_S M_B \begin{pmatrix}\theta_{C2}\\ \phi_{C2} - P_{BS}\end{pmatrix} - M_M \begin{pmatrix}0\\ P_{MC}\end{pmatrix}. \tag{4}$$

The matrix $M_i, i = M, C, S, B$, represents respectively, the heat transfer matrix of the metal layer, cap layer, superlattice layer, and buffer layer.

$$\begin{cases} P_{MC} = -S_{MC} I_e T_0 \\ P_{BS} = -S_{BS} I_e T_0 \\ \phi_{C1} = -\dfrac{\theta_{C1}}{Z_{K1}} \\ \phi_{C2} = \dfrac{\theta_{C2}}{Z_{K2}}. \end{cases} \tag{5}$$

S_{MC}, and S_{BS} are the relative Seebeck coefficients at the interfaces metal layer/cap layer and buffer layer/substrate which include both thermoelectric and thermionic contributions. I_e is the excitation current amplitude, and T_0 is the average temperature of the junction that we take equal to room temperature.

The top side metallic contact is modeled by a fin model which takes into account heat conduction via the SiN layer to the substrate and vice versa. Z_{K1} is the thermal impedance which describes heat leakage from the top side contact of the device. The current probe is supposed to be far away from the device, so that we can neglect the heating coming from it. Because the excitation is periodic, it follows that the temperature of the structure will also be periodic, having the same period, especially the junction temperature, which we can expand in the form of a Fourier series:

$$T_J = \overline{T_J} + \sum_{k=1}^{\infty} T_{kJ} \cos(k\omega t + \phi_k). \tag{6}$$

$\overline{T_J}$ is the average junction temperature, T_{kJ} and Φ_k are respectively the amplitude and the phase of the harmonic k. The Peltier heat power at the junction J is given by:

$$P_J = -S_J T_J I_e \cos(\omega t). \tag{7}$$

Taking into account relation (6), relation (7) becomes:

$$\begin{aligned} P_J &= -S_J \left[\overline{T_J} + \sum_{k=1}^{+\infty} T_{kJ} \cos(k\omega t + \phi_k) \right] I_e \cos(\omega t) \\ &= -S_J \overline{T_J} I_e \cos(\omega t) \\ &\quad - \frac{S_J I_e}{2} \sum_{k=1}^{+\infty} T_{kJ} \left\{ \cos\left[(k+1)\omega t + \phi_k\right] + \cos\left[(k-1)\omega t + \phi_k\right] \right\}. \end{aligned} \tag{8}$$

As we can see, the first harmonic depends mainly on the average junction temperature $\overline{T_J}$, but also on the amplitude T_{2J} of the second harmonic. In addition to the Peltier effect, the second harmonic depends on the Joule effect, which is a quadratic effect on current amplitude. At the first harmonic (the fundamental harmonic), the Peltier heat power takes the form:

$$P_J(1\omega) = -S_J \overline{T_J} I_e \cos(\omega t) - \frac{S_J I_e T_{2J}}{2} \cos(\omega t + \phi_2). \tag{9}$$

For small temperature variations, we can consider $\overline{T_J} \gg T_{2J}$. Relation (9) becomes:

$$P_J(1\omega)\# - S_J \overline{T_J} I_e \cos(\omega t). \tag{10}$$

This simplification allows us to have a completely linear model between Peltier heat power, current amplitude, and average junction temperature. For small current amplitudes, the average junction temperature deviates little from room temperature. For this reason the temperatures of both the metal/cap layer and buffer layer/substrate junctions are considered equal to room temperature $T_0 = 300$ K.

The substrate is thermally thick, and its effect will be contained in what is called the *impedance of constriction* Z_{k2}. This impedance results from the constriction of thermal flux lines when heat flows through the interface of two media of different geometries. In the

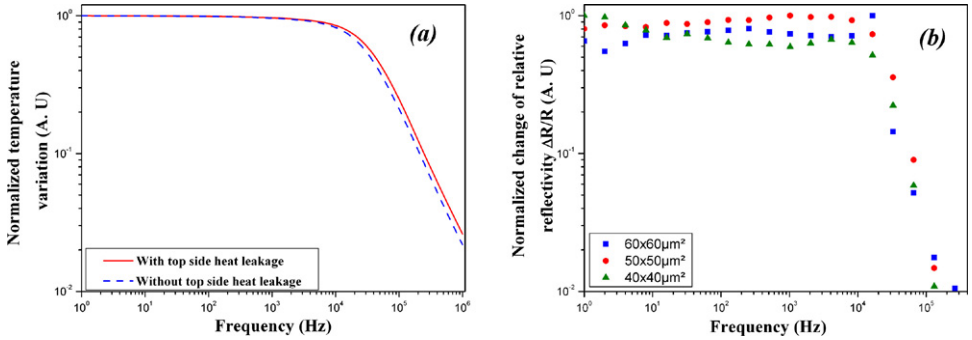

Fig. 3. (a) Normalized Peltier effect frequency response of the microcooler with (solid line) and without (dashed line) top side heat leakage. (b) Normalized experimental change of relative reflectivity $\Delta R/R$ for different microcooler sizes.

approximation of cylindrical geometry for both the microcooler and the substrate, the impedance of constriction for a uniform flux distribution on the contact disc $[0, r]$ is given by [5]:

$$Z_{k2} = \frac{8}{3\pi^2 \beta_s r \left(1 + \frac{8r}{3\pi}\sqrt{\frac{p}{\alpha_s}}\right)} \tag{11}$$

r is the radius of the contact disc between the two media, β_s, and α_s are thermal conductivity and diffusivity of the substrate respectively.

Cooling occurs when electronic current flows from the top to the bottom of the structure. Because the Seebeck coefficients of the metal layer are less than that of the superlattice and the Seebeck coefficient for the superlattice is smaller than that of the silicon substrate, both interfaces, metal/superlattice and superlattice/substrate, act in the same way, cooling or heating together. We find that cooling occurs if we use the $(-)$ sign in the expressions of P_{MC}, and P_{BS}, which are, respectively, the amounts of heat absorbed by the thermoelectric Peltier effect and thermionic effect at the interfaces metal layer/cap layer and buffer layer/silicon substrate.

5. Results and discussion

The resolution of Eq. (4) with respect to θ_{C1} gives the temperature variation of the top side surface of the microcooler. Fig. 3(a) shows the simulation of the temperature variation at the top side surface of the $40 \times 40\ \mu m^2$ microcooler as a function of the excitation frequency for a current amplitude $I_e = 0.5$ A in two cases: with and without top side heat leakage from the device. The simulation confirms experimental results already obtained by Dilhaire et al. [11], and which we report in Fig. 3(b). The time response of the microcooler is <8 μs, and is about 10^4 times faster than the conventional Bi_2Te_3 coolers. In fact, we found a cut-off frequency $F_{\text{cut-off}} > 20$ kHz, which decreases as the device size increases. Previous experimental results [12,13] have shown that this frequency is mostly independent of the device size. To check this result, we have done more simulations to study the behavior of the cut-off frequency with respect to several microcooler properties. Table 1 lists all parameters used in our simulation [3,14,15].

The frequency dependence of the microcooler thermal behavior is like a low-pass filter like most systems. So in the time domain we can write the temperature evolution as:

$$\Delta T(t) = \Delta T_m \left[1 - \exp\left(-\frac{t}{\tau_m}\right)\right]. \tag{12}$$

Table 1
Si/SiGe microcooler thermophysical properties used in the simulation

Layer	Metal	Cap	Superlattice Si/SiGe	Buffer	Substrate	SiN
Seebeck coefficient (μV/K)	8	250	220	220	540	//
Electrical conductivity (Ω^{-1} m^{-1})	8.84×10^6	6.25×10^4	6.25×10^4	5×10^3	5×10^4	0
Thermal conductivity (W/m/K)	65	9.6	8	6.1	148	1
Density (kg/m^3)	8336	2673	2663	2673	2329	3440
Specific heat (J/kg/K)	516	614	632	614	700	170

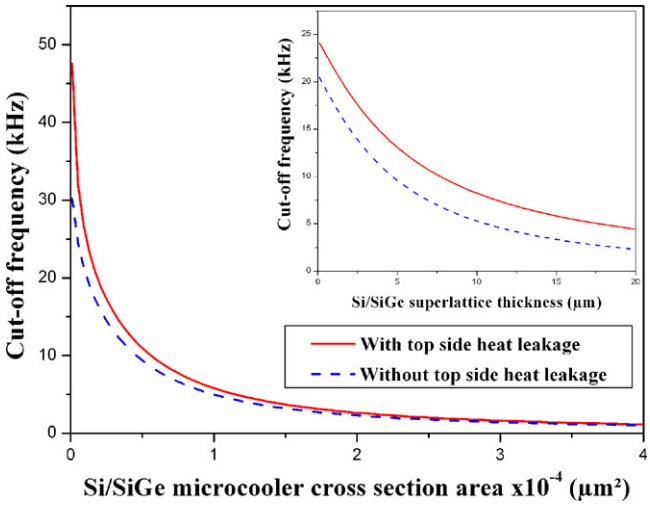

Fig. 4. Simulated variation of the microcooler cut-off frequency as a function of the microcooler cross section area and Si/SiGe superlattice thickness (the inset), with (solid line) and without (dashed line) top side heat leakage.

ΔT_m is the maximum cooling the device can achieve, and τ_m is its characteristic time response. The small value of τ_m is of great importance in many applications as mentioned in the introduction. Especially many biological and medical applications will be interested by the fast response of the microcoolers, in such a way that the time t_{Π} to achieve a desired temperature cooling Π is proportional to τ_m, and is given by:

$$t_{\Pi} = \tau_m \ln\left[\frac{\Delta T_m}{\Delta T_m - \Pi}\right]. \tag{13}$$

Π is the desired temperature cooling, giving by:

$$\Pi = \Delta T(t_{\Pi}). \tag{14}$$

The goal now is to find how to minimize the time response of the microcooler, or how to maximize the corresponding cut-off frequency as much as possible. Fig. 4 shows the simulation of the variation of the cut-off frequency of the Si/SiGe microcooler as a function of its cross sectional area in both cases: with and without top side heat leakage. As we can see the cut-off frequency decreases as the device area increases, which means that the time response increases. This is not surprising because heat dissipation becomes slow when the thermal mass increases,

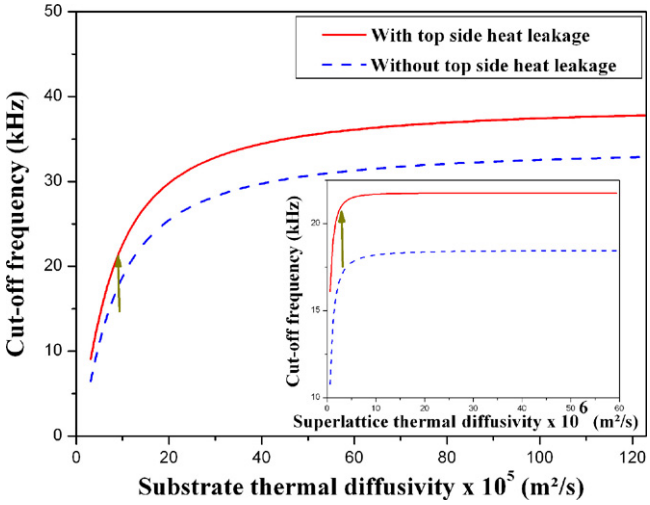

Fig. 5. Simulated variation of the 40 × 40 μm^2 size microcooler cut-off frequency as a function of substrate thermal diffusivity and Si/SiGe superlattice thermal diffusivity (inset), with (solid line) and without (dashed line) top side heat leakage.

and the latter increases by increasing the cross sectional area for a fixed device thickness. In the inset, we show the variation of the cut-off frequency of a 40 × 40 μm^2 device area as a function of the Si/SiGe superlattice thickness. Here also, the cut-off frequency decreases as the thickness of the superlattice layer increases; this is consistent with the previous analysis. In contrast with the experimental results, simulation shows a significant variation of the cut-off frequency as a function of the cross section area of the microcooler. In an experimental configuration [12,13], either the substrate response or the thermal mass of the heater partially hides the real response of the active microcooler layers. The TQM describes the heat transfer in each layer separately; the substrate acts only via the thermal impedance of the constriction at the interface buffer layer /substrate. This constriction resistance does not hide the response of the microcooler, which could explain the discrepancy between experiment and simulation.

The influence of the substrate thermal diffusivity and the Si/SiGe superlattice thermal diffusivity on the cut-off frequency is also studied. In fact this parameter is more relevant than thermal conductivity when considering dynamical behavior. Fig. 5 shows a simulation of the cut-off frequency of the Si/SiGe microcooler as a function of substrate thermal diffusivity and Si/SiGe superlattice thermal diffusivity (the inset) for a 40 × 40 μm^2 device considering two cases: with and without top side heat leakage. The arrows indicate the value of the cut-off frequency with actual device material properties, which is of the order of 21.7 kHz; this corresponds to a time response of the order of ∼7.3 μs.

Both behaviors are similar, as the thermal diffusivity of the substrate (superlattice) increases, the cut-off frequency increases. The explanation of this behavior is the same as above. In fact, when the thermal diffusivity increases, heat dissipation becomes faster: therefore, the time response decreases, and then the cut-off frequency increases. We can also see that a substrate with a thermal diffusivity value higher than 6×10^{-4} m^2/s will not improve the time response of the device very much. The influence of the superlattice thermal diffusivity seems negligible in comparison with that of the substrate. As shown in the inset, the cut-off frequency becomes insensitive to the thermal diffusivity of the superlattice after $\sim 1 \times 10^{-5}$ m^2/s.

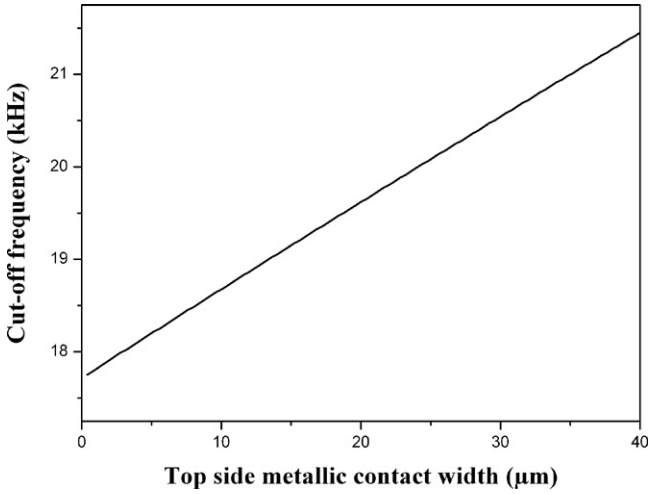

Fig. 6. Simulated variation of the $40 \times 40\ \mu m^2$ size microcooler cut-off frequency as a function of top side contact width.

As we can see in all of Figs. 3–5, the cut-off frequency decreases when the top side heat leakage is removed. This behavior is not surprising since in this case heat will be partially trapped inside the device and the only way to release it is through the substrate. The time response increases, and consequently the cut-off frequency decreases. This behavior is confirmed in Fig. 6 which shows the variation of the cut-off frequency of a $40 \times 40\ \mu m^2$ microcooler as a function of the top side contact width. The cut-off frequency increases linearly by increasing this width.

This preliminary study proves the benefit we can get by using a high thermal diffusivity substrate, and keeping the top side heat leakage. However these two parameters decrease the steady maximum cooling of the device [16], and thus it is necessary to find a compromise between steady-state and dynamical behaviors of the microcooler for better operation performance. The optimization will depend on the nature of the applications.

6. Conclusion

The large cut-off frequency of thin film microcoolers makes them very attractive for use in a temperature control feedback loop, as the short time scale for temperature stabilization is critical in sensitive optoelectronic or electronic applications. We presented simulation of the Si/SiGe microcooler cut-off frequency as a function of several material and device geometric parameters. The simulation included the effects of the substrate and the Si/SiGe superlattice thermal diffusivities, as well as the device cross sectional area and superlattice thickness. This preliminary study shows the benefit of a high thermal diffusivity substrate. Although we have concentrated on the superlattice properties, the cut-off frequency of the microcooler is proved to be sensitive to the properties of the entire device.

Acknowledgements

The authors would like to thank ‘La Région d’Aquitaine’, FEDER, Le Ministère de la Recherche (CPER), DARPA, DOE and Packard Foundation for supporting this work.

References

[1] D.M. Rowe, Handbook of Thermoelectrics, CRC, 1995.
[2] D. Vashaee, C. Labounty, X. Fan, G. Zeng, P. Abraham, J.E. Bowers, A. Shakouri, Proceedings of the SPIE-The International Society for Optical Engineering 4284 (2001) 139–144.
[3] D. Vashaee, J. Christofferson, Y. Zhang, A. Shakouri, G. Zeng, C. Labounty, X. Fan, J. Piprek, J.E. Bowers, E. Croke, Microscale Thermophysical Engineering 9 (2005) 99–118.
[4] Y. Ezzahri, S. Dilhaire, S. Grauby, L.D. Patiño-Lopez, W. Claeys, Y. Zhang, Z. Bian, A. Shakouri, The 24th International Conference on Thermoelectrics, 19–23 June, Clemson, SC, USA, 2005.
[5] D. Maillet, S. André, J.C. Batsale, A. Degiovanni, C. Moyne, THERMAL QUADRUPOLES: Solving the Heat Equation through Integral Transforms, John Wiley & Sons, 2000.
[6] L.D. Patiño-Lopez, Ph.D. Thesis, ON 2792, University Bordeaux 1, 2004.
[7] Y. Zhang, G. Zeng, R. Singh, J. Christoffersen, E. Croke, J.E. Bowers, A. Shakouri, The 21st International Conference on Thermoelectrics, 25–29 August, Long beach, USA, 2002, pp. 329–332.
[8] J.P. Douglas, Semiconductor Science and Technology 19 (2004) 75–108.
[9] A. Shakouri, E.Y. Lee, D.L. Smith, V. Narayanamurti, J.E. Bowers, Microscale Thermophysical Engineering 2 (1998) 37–47.
[10] G.D. Mahan, J.O. Sofo, M. Bartkowiak, Journal of Applied Physics 83 (1998) 4683.
[11] S. Dilhaire, Y. Ezzahri, S. Grauby, W. Claeys, J. Christofferson, Y. Zhang, A. Shakouri, The 23rd International Conference on Thermoelectrics, 17–21 August, La Grande Motte, 2003, pp. 519–523.
[12] A. Fitting, J. Christofferson, A. Shakouri, X. Fan, G. Zeng, C. Labounty, J.E. Bowers, E.T. Croke, ASME Heat Transfer Division Conference, IMECE, November 2001.
[13] A. Shakouri, Y. Zhang, IEEE Transactions on Components and Packaging Technologies 28 (1) (2005) 65–69.
[14] Y. Zhang, D. Vashaee, J. Christoffersen, A. Shakouri, G. Zeng, C. Labounty, J. Piprek, E. Croke, International Mechanical Engineering Congress and Exposition, 16th–21st November, Washington, DC, 2003.
[15] Y. Ezzahri, Ph.D. Thesis, ON 3090, University Bordeaux 1, 2005.
[16] Y. Ezzahri et al., (in press).